*In: Proceedings of 11th International Conference on Civil, Structural and Environmental Engineering Computing, Malta. September 2007*

**Paper Title:**

# The influence of finite element modelling parameters on the stress distribution in bolted glass connections

(The influence of modelling parameters on the stress distribution in glass connections)

**Authors:**
**Dr. Mauro Overend**
School of the Built Environment, University of Nottingham, UK.
**Dr. Ing. Iris Maniatis**
Whitbybird Engineers, London, UK.

## Abstract

Bolted glass is being increasingly used in buildings to enhance the 'transparency' of structures and to overcome the relatively small manufacturing sizes of thermally toughened glass plates. Despite their popularity there is a general lack of test date and design guidelines for these connections. This paper describes the research efforts in this area including the determination of glass strength and the influence of finite element modelling parameters on stress distribution. Guidelines for good practise modelling are provided.

**Keywords:** Bolted glass, glass finite element analysis, glass strength, glass connections

# 1 Introduction

For several years there has been a trend in architecture, to use glass not only as infill panels in the building envelope, but as load bearing elements in buildings such as glass floors, walls, staircases, beams and fins. This increasingly structural use of glass is particularly challenging for engineers who are called upon to design safe yet efficient glass structures. In order to achieve this, engineers must be able to determine the stresses imposed by the applied loads and support conditions as well as determining whether these stresses will result in the failure of the glass.

Another major challenge in glass construction is presented by the maximum manufacturing size of thermally toughened glass plates which is normally limited to 2.4m x 4.2m. This poses a limitation to the maximum size of uninterrupted structural glass element, therefore such elements are often composed of an assembly of several thermally toughened glass plates. The glass plates are connected together by specially developed stainless steel bolts and fixings that transmit the loads from one glass panel to another by in-plane bearing on the boltholes drilled into the glass.

Furthermore, in order to achieve the desired level of ‘architectural transparency’, the number of bolts and the overall size of the fixings are kept to a minimum.

These bolted connections cause high stress concentrations in glass and must therefore be designed with caution. However, there is a paucity of guidelines for designing bolted glass connections and engineers often rely on a ‘design-assisted-by -testing’ approach where the bolted connections are modelled in a commercial finite element analysis software and this is followed by prototype testing. However there are often large discrepancies between predicted strength values and the fracture strength obtained from the prototype testing.

This paper describes on-going research in this field that aims to use finite element analysis and the recent advances in glass failure prediction models to determine the strength of bolted glass connections in an accurate manner. In detail this paper describes the initial research effort which consists of a review of the mechanical properties of glass, the procedure for determining glass strength and the initial numerical investigation carried out to determine the influence of FEA modelling parameters on the stress distribution of bolted glass connections.

The ultimate aim of this research is to provide reliable simplified equations for the design of the more common types of bolted glass connections and to provide guidelines for the modelling and testing of bespoke bolted glass connections

# 2 Glass Properties and Applications

## 2.1 Mechanical properties of glass

Glass has been discovered more than 4000 years ago and used in buildings since Roman times. The developments and refinements of manufacturing techniques over the last few centuries have resulted in a wide range of distinct production processes, the descriptions of which is beyond the scope of this paper and are documented elsewhere [1], [2].

The float process, developed by the Pilkington brothers in the 1950’s, accounts for about 90% of the today’s flat glass production worldwide is shown schematically in Figure 1 and involves: (a) melting of the raw materials at 1550˚C which largely consist of Silica sand ($SiO_2$), Lime (CaO) and Soda ($Na_2O$); (b) floating of the molten glass at 1200˚C over a bath of molten tin; (c) gradually cooling the glass from 600˚C to room temperature in the annealing lehr to produce annealed glass. This process is followed by checking cutting, storing and subsequently by several possible permutations of off-line processes. Furthermore on-line coatings may be applied during the float process itself.

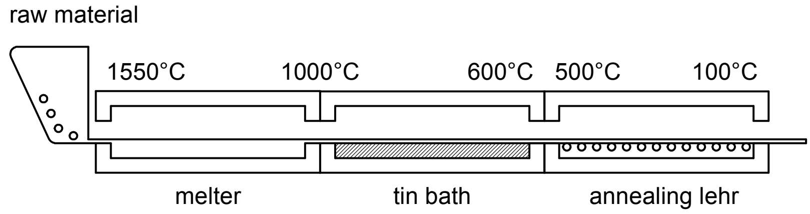

Figure 1 Float glass manufacturing process

The two stages in the production of glass that have a major influence on the strength and failure characteristics of the material are the solidification of glass that occurs at around 530°C and the post-processing of glass by heat treatment. The solidification of glass occurs by cooling to a rigid state before crystallisation can occur. The prevention of crystallisation, that is also responsible for the transparent nature of glass, produces a homogenous molecular structure without long-range order or slip planes that are a pre-requisite for ductile failure. Therefore glass exhibits almost perfect elastic isotropic behaviour.

Furthermore, handling, weathering and working (e.g. cutting drilling etc.) of the glass introduce atomically sharp randomly located flaws (known as Griffith flaws) on the glass surface. The stress at the tip of a flaw in a semi-infinite surface, shown in Figure 2, may be represented by:

$$\sigma_{tip} \approx k_{shape}\sigma_n (c/\rho)^{1/2} \tag{1}$$

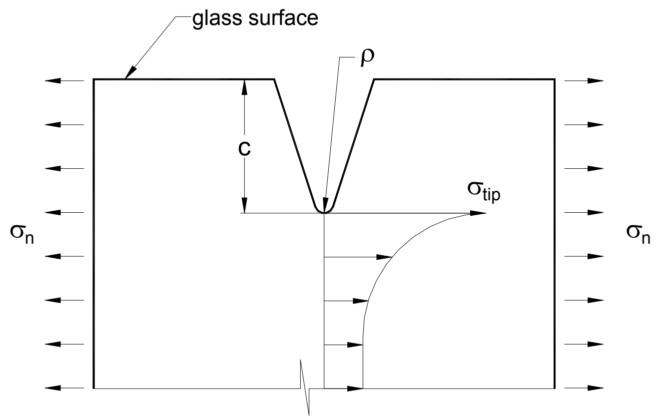

Figure 2 Idealised cross-section through surface flaw

Where $\sigma_n$ is the mean stress, $c$ is the flaw depth (or half the flaw length), $\rho$ is the radius of curvature of the flaw tip and $k_{shape}$ is a function of the flaw geometry ($k_{shape}$ =2 for a narrow ellipse). Due to its brittle nature a glass element fails as soon as the stress intensity at the tip of one of the flaws reaches its critical value and since the flaws are atomically sharp (i.e. $c >> \rho$) glass fails in tension at values below 100MPa which is several orders of magnitude below its theoretical molecular strength.

This phenomenon was conveniently described by Irwin [3] in terms of the stress intensity factor $K$ and its critical value $K_{IC}$. The stress intensity factor for mode I loading (opening mode) is given by:

$$K_I = \sigma_n Y (\pi c)^{1/2} \tag{2}$$

where $Y$ is a geometry factor that accounts for the crack geometry and the proximity of the boundaries.

When the critical stress intensity is reached (i.e. $K_I \geq K_{IC}$) the flaw grows rapidly at a speed of between 1.5mm/μs and 2.5mm/μs which is perceived as instantaneous failure. However, when the tensile stress intensity is below the critical stress (i.e. $K_{th} < K_I < K_{IC}$ ), flaws may grow very slowly (between $10^{-3}$ m/s and $10^{-7}$m/s in region I of Figure 3). The extent of this form of stress corrosion, termed sub-critical crack growth, is a function of several parameters, in particular the condition of the surface, the stress history (intensity and duration), the size of the stressed surface area, the residual stress and the environmental conditions [4], [5], [6], [7].

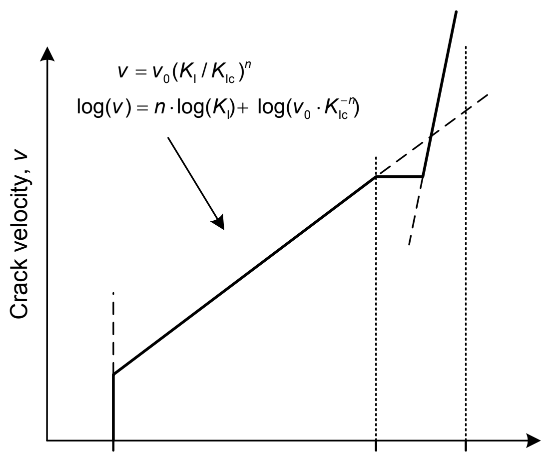


Figure 3 v-K relationship

In order to counteract any high tensile stresses, it is common practise to use tempered glass. During the tempering process the annealed glass is heated to approximately 650°C and subsequently cooled rapidly. This process induces a beneficial residual stress which places the outer surfaces of the glass in compression (Figure 4) In doing so, any externally applied stresses must overcome the pre-compression before the surface flaws can come into play. Standard surface pre-compressions in Europe range from 90MPa to 140MPa .Tempered glass also has the added advantage of failing into small relatively harmless dice rather than the sharp shards that characterise annealed glass failures.

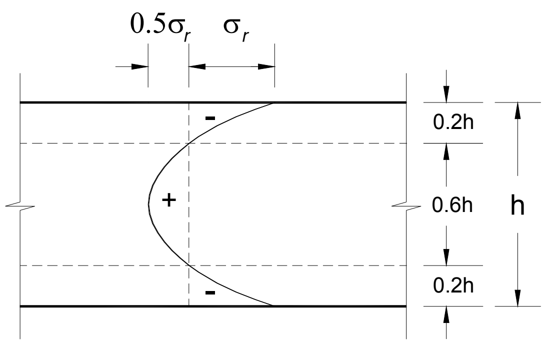


Figure 4 parabolic stress distribution induced by tempering process

## 2.2 Use of Bolted Glass in Buildings

During the last 50 years there has been a rapid evolution in the application of glass elements in buildings; from the linearly supported glazing associated with the curtain walls developed in the mid 20th century, to the patch plate friction fittings developed in the mid 1970's, to the bolted point supports developed in the 1980's and 1990's (figure 5). These developments, fuelled by the architectural requirements to increase the 'transparency' of glass structures tend to reduce the size, and eventually eliminate, the solid structures that support the glass. In doing so, the role of glass elements is transformed from small infill panels that resist local wind loads to structural glass where the panels contribute to the overall load-bearing capacity of the structure (figure 6).

The ubiquitous bolted glass connections, whether used in infill panel applications or for more structural applications are clearly not the most suitable type of connection for glass. Firstly, glass being a brittle material cannot redistribute local stress concentrations by yielding locally, thereby making bolted connections relatively inefficient from a structural point of view. Secondly, the surface flaws in glass caused by the drilling of holes and the distortions of the tempering stresses around holes mean that bolted connections are inducing the highest stress concentrations in the area of the glass panel which contains the most severe flaws. Bolted connections in glass therefore require a greater attention to detailing and much tighter fabrication and construction tolerances than similar connections in steel or timber structures.

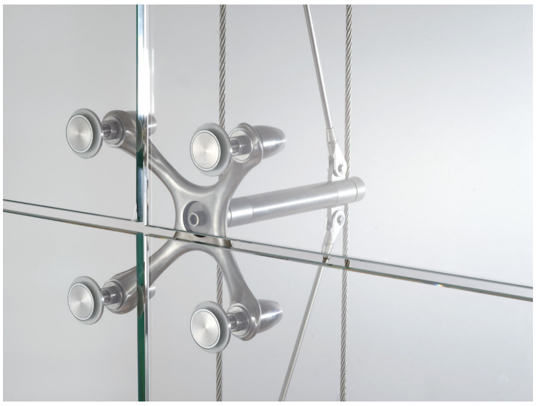

Figure 5 Image of typical bolted connection in glass

Figure 6 Example of load bearing glass fins with bolted connections

In spite of their shortcomings, bolted connections have a major aesthetic appeal and there is an increasing demand for these connections which is being met by a wide range of bolted glass ironmongery produced by several manufacturers around the world. In the absence of detailed design guidelines, predictions of the structural performance and the load-bearing capacity of these connections are normally undertaken by a combination of finite element (FE) analysis and prototype testing.

There is often a poor correlation between the strength predictions from FE analysis and the test results from the prototype testing. These discrepancies are due to the following:

1. Incorrect strength prediction arising from the adoption of over-simplified glass failure prediction models.
2. Incorrect stresses arsing from errors in FE modelling.

These are discussed in section 3 and section 4 respectively.

# 3 Procedure for Determining the Strength of Glass

Determining the strength of glass in an accurate manner is a non- trivial task because as described in section 2, the strength of glass is often governed by sub-critical crack growth, which is in turn dependant on the severity of the flaws, the stress history, the surface area and environmental factors. In addition the exact size, the location and orientation of the critical flaw is rarely known so these factors must be expressed statistically. This phenomenon is best explained by the fact that testing of nominally identical glass specimens will results in a wide scatter of strength data and the origin of the failure rarely coincides with the point of maximum stress, but is a combination of the surface stresses and the severity of the randomly located surface flaws.

Numerous design recommendations have been developed to enable the engineer to select the minimum glass thickness that can safely resist the estimated lateral wind load. These recommendations range from rules of thumb and guidelines based on the simple, yet less accurate, maximum stress failure criterion to the more rigorous design methods based on fracture mechanics and failure statistics [4], [8], [9], [10].

An accurate characterisation of the tensile strength of glass may be derived from linear elastic fracture mechanics as shown in Fischer-Cripps & Collins [5] and extended by Overend *et al.* [7] such that:

$$\sigma_f = k_{\mathrm{mod}}\sigma_s + \sigma_r / \gamma_v \quad (3)$$

where $\sigma_f$ is the instantaneous tensile strength of glass. $k_{mod}\,\sigma_s$ is the strength of glass without surface pre-compression (i.e. annealed glass). This term is composed of the instantaneous failure stress of annealed glass, $\sigma_s$ and the stress corrosion ratio, $k_{mod}$ . The stress corrosion ratio takes into account the load duration and the surface area of the glass and typical values listed in prEN 13474 are 0.72, 0.36 and 0.27 for short, medium and long term loads respectively. Further information on the stress corrosion ratios may be found in Haldimann [6] and Overend [11].

The term $\sigma_r/\gamma_v$ is the strength contribution provided by the tempering process in which $\sigma_r$ is the induced surface pre-compression. Generally, 90MPa $\leq \sigma_r \leq$ 140MPa in Europe and $\sigma_r \geq$ 69MPa in North America; $\gamma_v$ is a partial safely factor depending on the quality control of the tempering process (typically, $1.5 \leq \gamma_v \leq 2.3$). It is important to note that the surface pre-compressions induced by the tempering process are distorted close to free edges and holes in the glass [12]. Therefore the magnitude of $\sigma_r$ depends on the location under consideration as well as quality control of the tempering process.

The instantaneous tensile strength, $\sigma_f$, obtained from equation (3) is valid for a glass element which is subjected to a uniform stress across its surface. This is clearly unlikely to occur in practise, it is therefore necessary to transform the actual stress field on the glass surface to an equivalent uniform stress, (which is the weighted average of the principal stresses on the surface) and may be calculated from:

$$\sigma_p = \left[ \frac{1}{A} \int_{area} \left( c_b \sigma_{\max} \right)^m dA \right]^{1/m} \quad (4)$$

where $A$ is the total surface area, $dA$ is the area of the subdivision under consideration, $\sigma_{max}$ is the major principal tensile stress within the subdivision, m is the surface strength parameter (typically $m$ = 7.3) and $c_b$ is the biaxial stress modification factor obtained from Beason & Morgan [4] or may conservatively be taken as unity. The full derivation of this equation is shown in Overend et al. [7] and is omitted here for brevity.

A safe design is achieved by then ensuring that:

$$\sigma_f \geq \sigma_p \quad (5)$$

The alternative maximum stress approach is often used when designing tempered glass due to its simple application. In this approach the strength of glass is solely derived from the compressive residual stresses i.e. the inherent strength of the annealed glass is ignored. This conservative approach simplifies the strength calculations by eliminating the first part of the right hand side expression in equation (3) therefore:

$$\sigma_f = \sigma_r / \gamma_v \quad (6)$$

In this case a safe design is achieved by ensuring that:

$$\sigma_f \geq \sigma_{\max} \quad (7)$$

The maximum stress approach is often regarded as too conservative and a general failure prediction model that takes the full stress distribution into account, such as the one described by equation (3) and equation (4), is preferred. However the surface strength parameter, *m*, required for this design is derived from data of as-received, naturally weathered and artificially abraded glass rather than for the more severe flaws associated with drilling of the holes.

# 4 Numerical Modelling

## 4.1 Introduction

Bolted connections cause high stress concentrations in the glass which must be predicted with a high degree of accuracy in order to design bolted glass assemblies in a safe and efficient manner.

In order to avoid unexpected stress concentrations, the design model must account for all relevant aspects and be analysed thoroughly. A good structural model of a glass structure should account for conventional actions due to load, temperature differences, imposed deformations and constraints, as well as the detailed geometry, the stiffness of all components including support bracketry and fixings as well as fabrication / installation tolerances including out of plane distortions and closeness of fit.

It is possible to predict both the stress distribution and the probability of failure numerically by means of non-linear Finite Element Analysis (FEA). However the results obtained from such FEA are sensitive to a wide range of modelling parameters such as mesh geometry, element type, non-linear solution, contact description etc.

The ensuing parts of this section identify the modelling parameters and discuss their influence on the results obtained from FEA. Some guidelines that help ensure good FE modelling are also provided.

## 4.1 Verification Methods

In order to evaluate the FEA model and exclude unsuitable models a verification is necessary. The verification can either be performed by means of an analytical solution - if available - or by experiment. For verification purposes the modelling parameters should be examined individually in order to evaluate their respective influence on the overall results. The Finite Element Analyses within this study were carried out with the program Nastran for Windows (N4W).

A sensible preliminary test for determining the adequate mesh geometry is to model a glass plate with a circular hole subjected to a uniform tensile stress field (figure 7). The resulting maximum tensile stresses present around the hole may be compared with the following analytical solution:

The nominal stress $\sigma_N$ is defined as:

$$\sigma_N = \frac{p \cdot 2b}{2(b-a)t} \tag{8}$$

In the case that *a* is only slightly smaller than *b* (Figure 7), Pilkey [13] gives a formula:

$$\sigma_\theta \max = K\sigma_N \tag{9}$$

where the stress concentration factor $K$ is

$$K = 3,00 - 3,13\left(\frac{a}{b}\right) + 3,66\left(\frac{a}{b}\right)^2 - 1,53\left(\frac{a}{b}\right)^3 \tag{10}$$

The maximum tensile stress occurs perpendicular to the load direction. For a given element type both the mesh geometry and mesh density should be modified until the FEA results converge to the analytical solution.

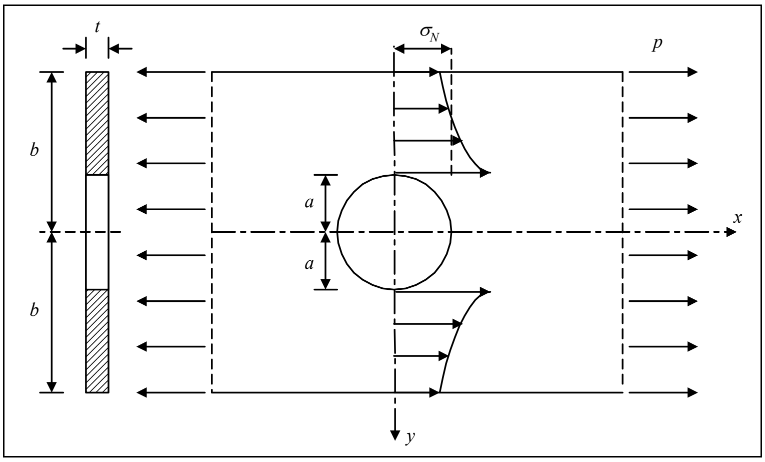


Figure 7 Panel with a width of *2b* and a hole of radius *a* under tensile stress

To verify the contact approach necessary for a bolted connection, both the plate and bolt have to be modelled. Analytical functions for the contact stress distributions have been treated by many authors [14], [15], [16], [17]. The most precise analytical approximate solution is obtained for a linear-elastic connection in an infinite panel, whereby bolt and panel consist of identical materials and the contact is assumed to be frictionless. A detailed explanation is given in [18]. In the following the formulations of Persson [19] are used as they include the deformation conditions in the contact area between panel and bolt (Figure 8, fFigure 9). The following equations are based on the assumption that only in-plane stresses result and that the surfaces are frictionless. Persson's approach is valid both for clearance between bolt and hole ( $\Delta R > 0$ ) and if the bolt fits in the hole ( $\Delta R = R_2 - R_1 = 0$ ).

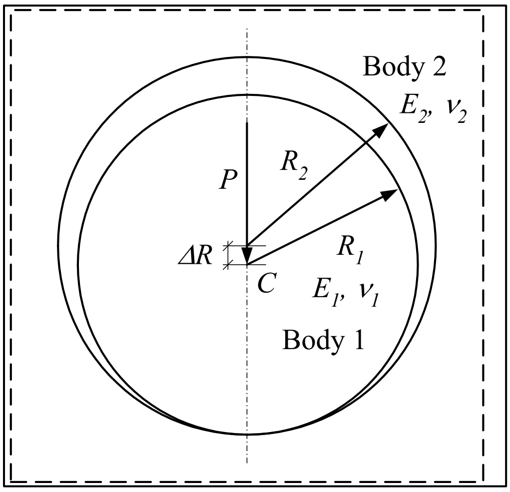


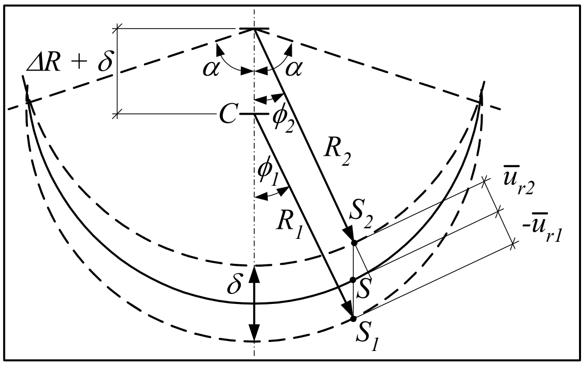


Figure 8 Infinite panel with a bolt in a conforming hole

Figure 9 Deformation in the contact area

For the case $E_1 = E_2$ or $\nu_1 = \nu_2$, i.e. both bodies have the same material properties, the tangential stress $p_\phi(\phi)$ on the contact surface of the glass panel (body 2) can be determined in closed form:

$$p_\phi(\phi) = \frac{P}{a}\left(-q(y) + \frac{3-\nu_2}{2\pi}\cos\phi + \frac{\ln(z^2+1)+2z^4}{\pi z^2(z^2+1)}\right) \tag{11}$$

$$q(y) = \frac{ap_r(\phi)}{P} = \frac{2}{\pi\sqrt{z^2+1}}\frac{\sqrt{z^2-y^2}}{1+y^2} + \frac{1}{2\pi z^2(1+z^2)}\ln\frac{\sqrt{z^2+1}+\sqrt{z^2-y^2}}{\sqrt{z^2+1}-\sqrt{z^2-y^2}} \tag{12}$$

$z = \tan\frac{\alpha}{2}$ $\alpha$ is the semi-angle of the contact segment (for $\Delta R = 0$ $\alpha$ =90°)

$y = \tan\frac{\phi}{2}$; $\phi$ is the contact angle

$a$ hole or bolt radius

For the verification it is further assumed that between bolt and hole no clearance occurs, i.e. $\Delta R = 0$.

In addition experimental investigations (Figure 10, figure 11) should be carried out to verify the Finite Element Analyses and to investigate the effect of other parameters that are overlooked in the analytical methods e.g. friction, material non-linearity or eccentric loading.

Several strain gauges should be placed strategically round the edge of the hole to capture the strains necessary for verification purposes. A detailed description of a test set-up and procedure can be found in Maniatis [18].

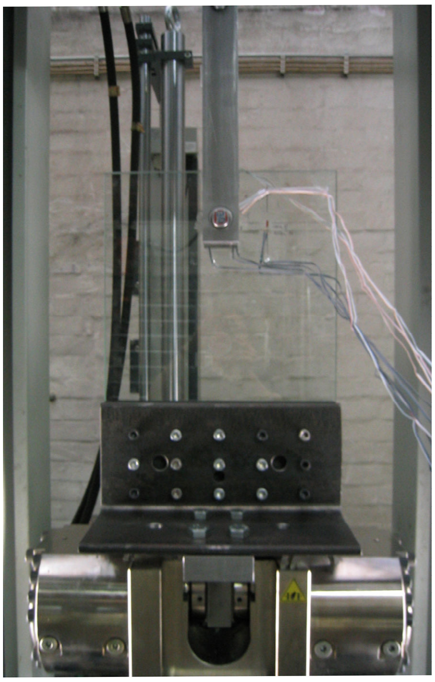
Figure 10 Example of a test-rig

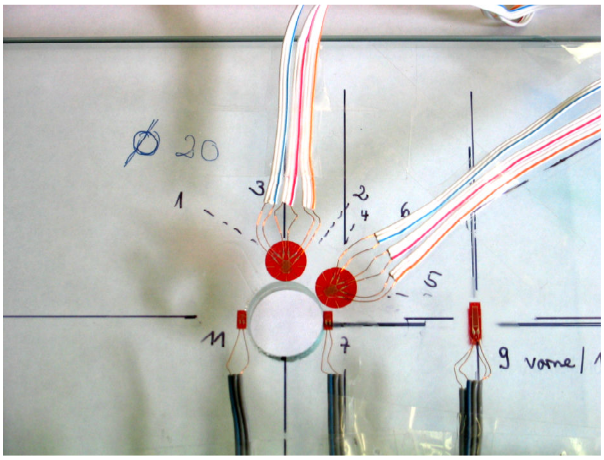

Figure 11 Position of strain gauges on the specimen

## 4.2 Parameter Study and Influence on the Stress Distribution

### 4.2.1 Mesh Geometry and Element Types

Within the FE modelling process the first important parameter is determining a reasonable mesh geometry and density around the hole. Studies by Maniatis [18] and Mano [20] were carried out where different mesh geometries were compared. In Figure 11 models with automatically meshed elements, manually meshed triangular elements, and manual meshed quadrilateral elements are compared (from left to right). The element types consisted of linear quadrilateral thin plate elements (CQUAD4) and linear triangular thin plate elements (CTRIA3).

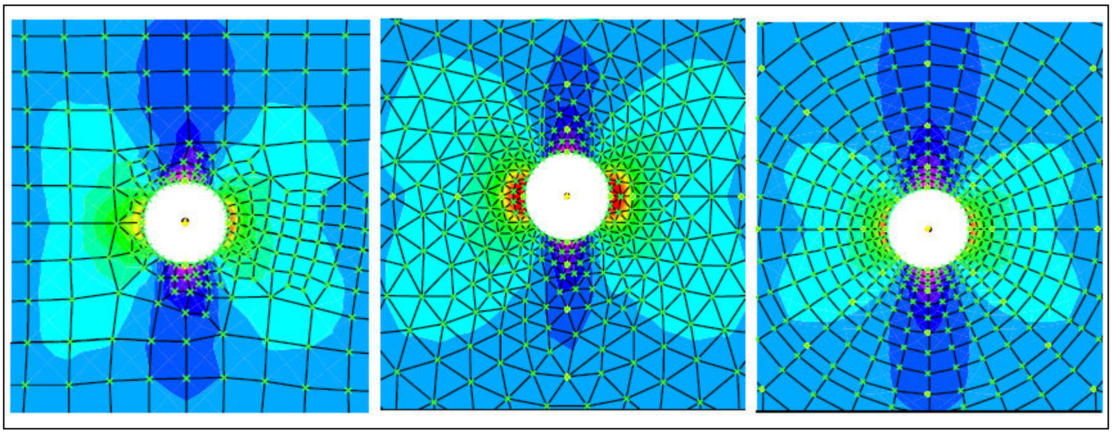

Figure 11  Comparison of meshing

The manually meshed model with quadrilateral elements provides maximum tensile stress, which appears at 90° to the direction of the applied load. The deviation from the theoretical tensile stress is $\Delta\sigma_{max}$= 1.2%. The automatically meshed plate shows a similar maximum tensile stress value to that given by the manually meshed quadrilateral elements but this is purely coincidental as this model results in an asymmetric stress distribution with variations in the maximum tensile stresses from one side of the hole to another. The model with the triangular mesh provides a relatively stiff model with maximum stresses in excess of the theoretical values. On this basis, only the manually meshed model with quadrilateral elements is adopted for further FEA analyses.

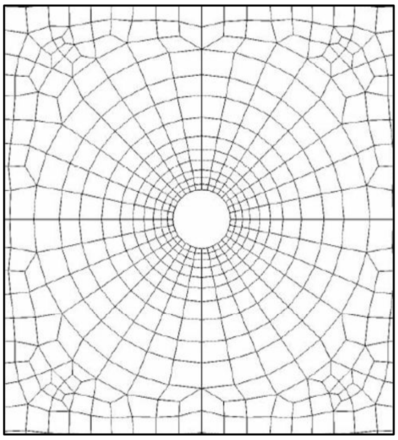

Figure 12  Mesh geometry around the hole

Further analysis showed that 32 elements in circumference of the hole give adequate results when comparing them with an analytical solution. Furthermore the number and geometry of the elements in radial direction have a noticeable influence on the stress gradients. A suitable size ratio of 1:1.5 between adjacent elements was found to yield accurate results. Figure 12 gives an example of an typical mesh geometry constructed from these recommendations.

Using plate and solid elements in N4W the nodal displacements and the rotations are calculated in the corner nodes and in the centroid of the element. Generally, the most accurate values are obtained in the centre of the element. When examining the stress distribution around holes, it is necessary to determine the stresses at the edges of the elements where the maximum stresses occur as they decrease very rapidly with increasing distance from the hole. Therefore it is important to use the pure "nodal" values without averaging them for the output instead of using "element" values which calculate the mean value of the linked nodes and result in significantly lower stresses.

When using plate elements it is not possible to determine the stress distribution across the thickness. Therefore, three dimensional solid elements of the type linear hexahedral (CHEXA) were used and the results where compared to those obtained from the 2-D plate elements and the analytical solution.

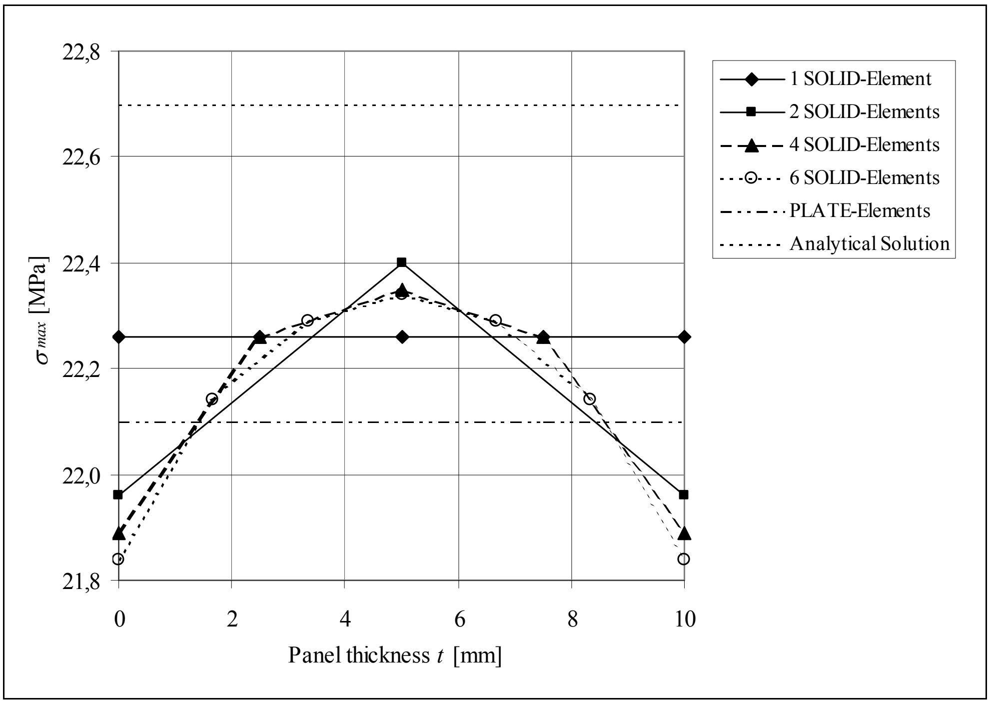


Figure 13 Stress distribution across plate thickness

Figure 13 shows the stress distribution alternatively modelled with 1, 2, 4 and 6 solid elements across the thickness. For all models the circumference of the hole was described by 32 elements. It can be seen that the stress distribution does not change significantly having 4 or more elements. The stress distribution also shows that the maximum occurs on the midplane of the plate and decreases towards the surfaces. This phenomenon is not detectable when modelling with plate elements which results in an small underestimation of the tensile stress values.

### 4.2.3 Contact

After determining the mesh geometry and the element type, the parameters of the contact algorithm were investigated. Failing to include a description for the contact of the bodies (i.e. glass plate and bolt) would cause the two to penetrate one another during the FE-analysis.

In general there are two necessary steps in order to detect whether contact takes place or not. One is the global search for contact and the other is setting up local kinematic relationships. For discretization of the contact several methods exist.

In N4W the contact is defined purely on nodal basis, where element nodes have to match each other at the contact interface (Figure 14). N4W provides "GAP"-elements which simulate the node-to-node contact. It is used to represent surfaces or points which can separate, close, or slide, relative to each other. Node-to-node contact can only be assumed if two deformable bodies have only small changes in the geometry so that no large slip can occur at the contact interface. The "Penalty-Method" is used for the numerical representation.

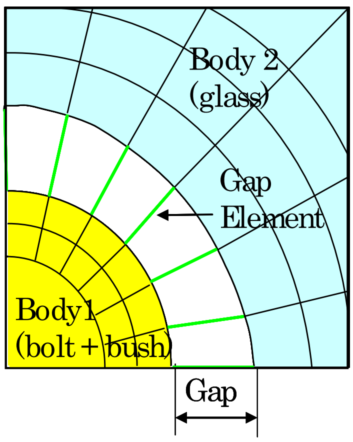


Figure 14 Contact interface

The "Penalty"-Method is used to simulate the stiffness between two degrees of freedom and depending upon the combination of materials and the geometry the compression stiffness has to be changed.

"Penalty"-values are introduced to avoid penetration and to cause friction between two points. Problems appear in case that the "Penalty"-values are not chosen correctly. The success of this method therefore depends on the chosen "Penalty"-values and is a compromise between accuracy and numerical power [21]. If the GAP is closed the axial stiffness $K_a$ has a large value relative to the adjacent structure ($K_a$ denotes the "Penalty"-value of the stiffness). $K_a$ should be chosen at least to be three orders of magnitude higher than the stiffness of the neighbouring grid points. A much larger $K_a$ value may slow down convergence or cause divergence, while a much smaller value may result in an inaccuracy. Therefore it is recommended to execute a convergence examination, before the "Penalty"-values (compression stiffness) are determined. Figure 15 gives an example where the influence of compression stiffness on the maximum compression stresses $\sigma_{min}$ for the material combination Aluminium (body 2, i.e. bush) and glass (body 1) is shown.

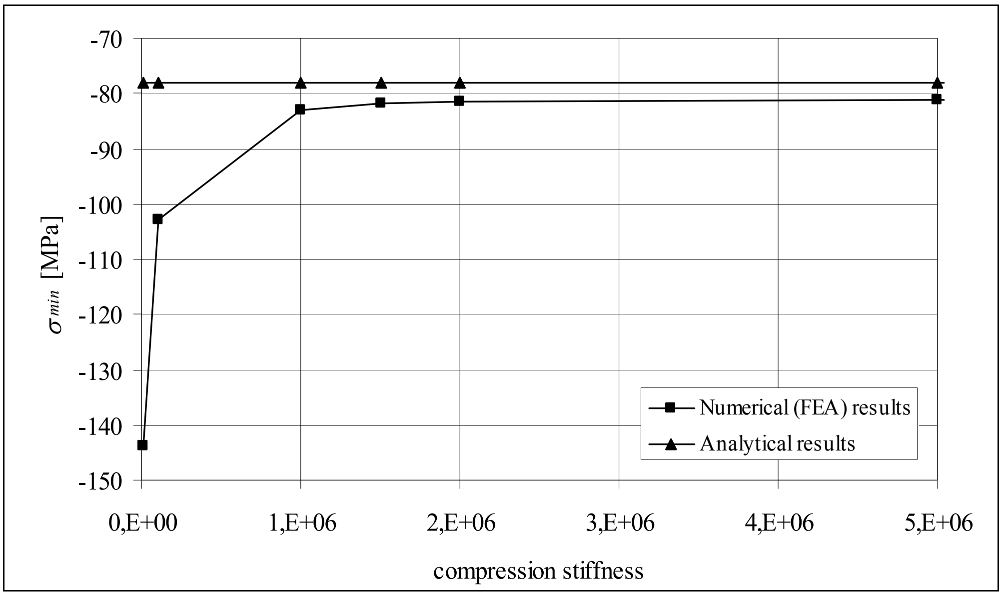


Figure 15 Influence of the compression stiffness for material combination glass-aluminium

As shown in Figure 15 the maximum compressive stresses $\sigma_{min}$ finally approach the analytical solution asymptotically after attaining a certain value of compression stiffness. If the chosen compression stiffness is too small, the results may deviate significantly. By increasing the compression stiffness the computation time increases and additionally convergence problems may occur.

A detailed convergence study was carried out by Maniatis [18] and Mano [20]. Compared with the analytical solution satisfying numerical results could be achieved when carrying out the convergence criteria for the neat-fit condition ($\Delta R$ = 0). Executing nonlinear analyses, it is generally recommended to apply the load in several increments, otherwise convergence problems may occur. Within these studies the load was applied in 10 increments. To solve the nonlinear equation systems the "Full *Newton-Raphson*-Iteration" was used.

Additionally it should be noted here that if a bush or liner exists between the bolt and the glass surface, this should be modelled with more than one element in the radial direction otherwise the deformation of the bush cannot be represented properly and will consequently provide wrong locations of the maximum compression.

# 5 Conclusion

There is a lack of published guidelines for designing bolted glass connections. This paper reviewed the two key steps that are necessary for design bolted glass in an accurate manner, namely, the correct characterisation of glass strength and the correct modelling and interpretation of results form FEA.

With respect to glass strength, although safe, the maximum stress approach is not appropriate for accurate calculations and a failure prediction model that accounts for flaw severity, stress history, stress distribution and environmental conditions should be adopted.

The initial modelling parameters investigated were found to have a major influence on the stress distribution. From these investigations the main good practise modelling guidelines are:

1. A minimum of 32 linear quadrilateral elements should be used to describe the circumference of the hole.

2. Solid elements should be used to determine the stress distribution across the glass thickness. This is particularly useful in asymmetric connections such as countersunk bolts.

3. A realistic contact model is time consuming, but may be achieved by using nonlinear contact algorithms (e.g. with gap elements). This approach requires some attention, particularly in the selection of the compression stiffness of the gap elements.

Future work in this area includes reviewing the performance of other commercially available software for modelling of bolted glass connections and combining the results obtained from FEA with the glass failure prediction model to provide reliable design formulas and guidelines for designing bolted glass connections.

## References


[1] Button D. and Pye B. (eds.), ‘Glass in Building’, Butterworth Architecture, UK, 1993.

[2] Rawson H. ‘Glasses and their Applications’, The Institute of Metals, London, 1991.

[3] Irwin G.R. ‘Fracture’. In: ‘Handbuch der Physik – Vol. 6’, Springer Verlag, Berlin, 1958.

[4] Beason W.L. and Morgan J.R. ‘Glass Failure Prediction Model’, ASCE J. Struct. Eng., 110(2): 197-212, 1984.

[5] Fischer-Cripps A.C. & Collins R.E. ‘Architectural glazings: Design standards and failure models’, Building and Environment, 30, 1, 29-40, 1994.

[6] Haldimann, M. ‘Fracture Strength of Structural Glass Elements – Analytical and Numerical Modelling, Testing and Design’. EPFL Thesis No 3671, Ecole Polytechnique Fédérale de Lausanne (EPFL), 2006

[7] Overend M, Parke GAR, Buhagiar D. Predicting failure in glass – A general crack growth model. ASCE J. Struct. Eng. FORTHCOMING August 2007.

[8] CAN/CGSB - 12.20.M89, ‘Structural design of glass for buildings’, National Standard of Canada, Canadian General Standards Board, 1989.

[9] ASTM E 1300–04. Determining Load Resistance of Glass in Buildings. Philadelphia, USA, 2004.

[10] prEN 13474-3:2007. Unpublished Draft. Glass in building - Determination of the strength of glass panes - Part 3: General method of calculation and determination of strength of glass by testing. CEN.

[11] Overend M. “The Appraisal of Structural Glass Assemblies.” PhD Thesis, University of Surrey, UK, 2002.

[12] Laufs W, and Sedlacek G. Stress distribution in thermally tempered glass panes near the edges, corners and holes; Part 2. Distribution of thermal stresses. Glass Science and Technology 1999; 72(2), 42-48.

[13] Pilkey, W. D. "Peterson's Stress Concentration Factors", John Wiley & Sons, Inc. 1997.

[14] Frocht M.M, Hill H.N. "Stress Concentration Factors Around a Central Circular Hole in a Plate Loaded Through Pin in the Hole". Journal of Applied Mechanics, Vol. 62, 1940, pp. A5-A9

[15] Theocaris, P.S. "The Stress Distribution in a Strip Loaded in Tension by Means of a Central Pin". Journal of Applied Mechanics Vol. 23, 1956, pp. 85-90.

[16] Girkmann K. "Flächentragwerke". Springer Verlag Wien - New York 1963.

[17] Gladwell G.M.L. "Contact problems in the classical theory of contact mechanics". Sijthoff & Noordhoff International PublishersB.V., Alphen aan den Rijn, 1980

[18] Maniatis, I. "Numerical and Experimental Investigations on the Stress Distribution of Bolted Glass Connections under In-Plane Loads", PhD Thesis Technische Universität München, Berichte aus dem Konstruktiven Ingenieurbau Nr. 1/06

[19] Persson A. "On the stress distribution of cylindrical elastic bodies in contact", Chalmers Tekniska Hogskola, Göteburg 1964
[20] Mano T., "Analysis of Bolted Pin Connections in Glass Structures". Master Thesis Chair of Steel Structures, Technische Universität München 2005
[21] Lee S.H., MSC/Nastran "Handbook for Nonlinear Analysis", Version 67. The McNeal-Schwendler Corporation, Los Angeles, Ca. 1992.